

Curie Point Depth Variations Derived from Aeromagnetic Data and the Thermal Structure of the Crust at the Zone of Continental Collision (South-East Cameroon)

Alain Narcisse S. Feumoe^{1,2} and Théophile Ndougsa-Mbarga^{3,4}

¹Department of Physics, Faculty of Science, University of Yaoundé I, P.O. Box 812 Yaoundé, Cameroon.

²Bureau de Recherches d'Etudes et de Contrôles Géotechniques (B.R.E.C.G), PO Box 7883 Yaoundé, Cameroon.

³Department of Physics, Advanced Teacher's Training College, University of Yaoundé I, P.O. Box 47, Yaoundé, Cameroon.

⁴School of Science, Technology and Geosciences, University of Yaounde I, Yaounde Cameroon.

(Received: Oct, 2014; Accepted: Aug 17, 2017)

Abstract

We have examined the thermal structure of the crust across the Congo Craton in South-East Cameroon using the Curie point depth (CPD) estimates and compared these results with the thickness of crust in the study area. The CPD estimates from four overlapping area vary from 20.0 to 25.0 km. The deeper CPDs are found corresponding to the Precambrian (Congo Craton) in the basement having lower heat flow and the shallow CPDs correspond to the metamorphic (Pan-African or mobile belt). The geothermal gradient varies between 23 and 29 °C.km⁻¹, while the few low heat flow values range from 57 to 72 mWm⁻². Thermal conductivity values in the region vary between 2.1 and 2.7 Wm⁻¹°C⁻¹ based on the constant temperature at the CPD. These results are consistent with the existing geothermal and geotectonic regime in the area. Spectral analysis of the aeromagnetic data in conjunction with heat flow values reveals an almost inverse linear relationship between the heat flow and CPD. The study has shown possible geothermal resources in the study area. In view of that, the results obtained from this study could be very important for geothermal exploration.

Keywords: Aeromagnetic data, Spectral analysis, Curie point depth, geothermal heat flow, geothermal gradients

1 Introduction

The study area, which lies in the Congo Craton between latitudes 2° to 3° N and longitudes 13° to 15° E, is one of the areas of the world that has preserved the earliest formed crust. Active deformation of this area is well controlled by the Eburnean orogeny (Feumoe *et al.*, 2012). The evolution is constrained by the continental collision between the Congo Craton and the mobile belt (Poidevin, 1983; Nzenti *et al.*, 1984; Penaye *et al.*, 1993; Trompette, 1994; Castaing *et al.*, 1994; Abdelsalam *et al.*, 2002; Basseka, 2002). This active collision marks the subduction of the Congo Craton under the Pan-African belt and the over thrusting of the Pan-African units onto the Craton of

about 50 to 150 km (*Manguelle-Dicoum et al.*, 1992; *Tadjou et al.*, 2009; *Shandini et al.*, 2010). This event can reveal the presence of geothermal environment via faulted structures. Curie point depth (CPD) is used in this research to analyse transition depth of magnetite. Generally, rocks are non-magnetite at a temperature greater than the temperature at the CPD of magnetite *Stampolidis and Tsokas* (2005). One of the tools of investigating the thermal framework via aeromagnetic studies is spectral analysis. This technique was adopted to analyze the CPD around Congo Craton in south-eastern Cameroon.

Thermal structure of the crust determines the modes of deformation, depths of brittle and ductile deformation zones. In the study area, the dense vegetation cover complicates direct geological and geophysical studies. The determination of the thermal structure of this region can be done without in-situ measurements for example with the regional aeromagnetic data and the estimation of the CPD. The CPD is the depth at which the dominant magnetic mineral in the crust passes from a ferromagnetic state to a paramagnetic state under the effect of increasing temperature (*Nagata*, 1961). Thermal structure of the crust involving CPD estimations have been published for various tectonic settings (*Vacquier and Affleck*, 1941; *Smith et al.*, 1974, 1977; *Bhattacharyya and Leu*, 1975; *Byerly and Stolt*, 1977; *Shuey et al.*, 1977; *Blakely and Hassanzadeh*, 1981; *Connard et al.*, 1983; *Okubo et al.*, 1985, 1989; *Blakely*, 1988; *Okubo and Matsunaga*, 1994; *Hisarli*, 1996; *Banerjee et al.*, 1998; *Tanaka et al.*, 1999; *Badalyan*, 2000; *Dolmaz et al.*, 2005; *Bansal et al.*, 2010).

Surface lineaments around the study area and their influence on the hot springs manifestations along its margins have not been previously investigated. The depth to the heat sources which could provide information on the thermal structure has not been investigated either. In this research, the thermal structure around Congo Craton, in south-eastern Cameroon was investigated in order to explore the geothermal potential using aeromagnetic data.

2 Geological and tectonic setting

The area under study lies in the South-East Cameroon and is made up of two geotectonic units: the Neoproterozoic mobile belt in the northern part that is represented by the Yaoundé domain and the Ntem Complex in the southern part, which is the north-western corner of the Congo Craton (Fig. 1).

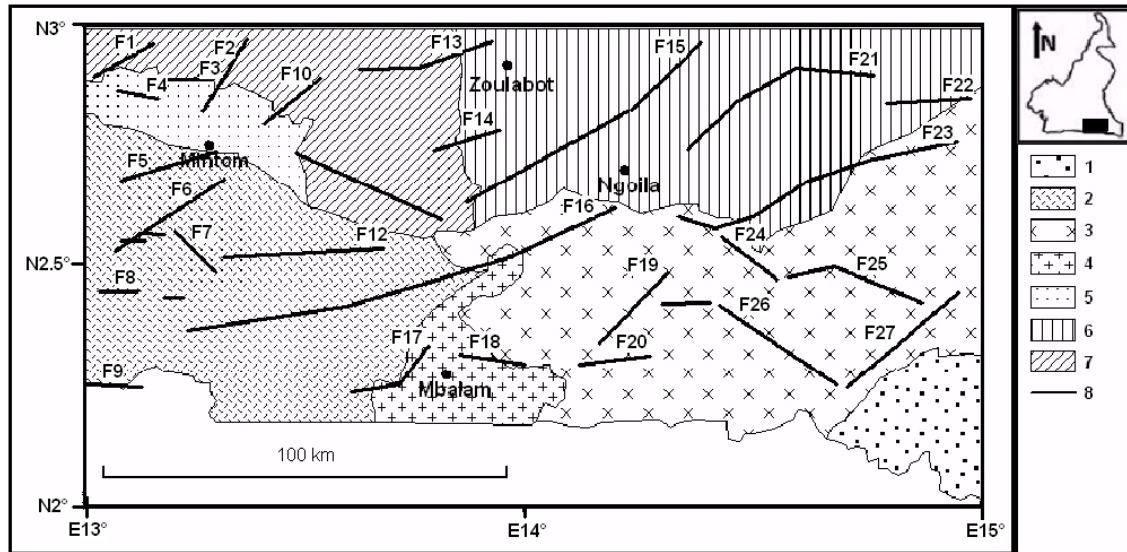


Fig. 1. Geological sketch map of the study area (modified after *Feybesse et al.*, 1987; *Ndougsa et al.*, 2012). Legend: 1. Mouloundou tillite, 2. Ntem unit, 3. Lower Dja series, 4. Mbalam series, 5. Upper Dja series, 6. Yokadouma series, 7. Mbalmayo-Bengbis series, 8. Major faults (F₁-F₂₇).

The Yaoundé domain is a huge allocthonous nappe unit that is thrust southward onto the Congo Craton. This domain belongs to the Pan-African belt in the north and includes the Mbalmayo-Bengbis and Yokadouma series. It comprises low-to-high-grade garnet-bearing schists, gneisses and orthogneisses metamorphosed under a medium to high pressure metamorphism reaching the granulite facies.

The Ntem Complex represents the north-western part of the Congo Craton in Central Africa and is very well exposed in southern Cameroon (*Maurizot et al.*, 1985; *Basseka*, 2002). The Ntem complex is made up dominantly of Archean rocks with some reworked material that formed in Early Proterozoic times (*Tchameni*, 2000; *Tchameni et al.*, 2001). It is divided into two main structural units: the Mbalam Unit to the central part and the Ntem Unit in the south-western area. The Ntem Unit is dominated by massive and banded plutonic rocks of the charnockite suite and by intrusive tonalites, trondhjemites and granodiorites. Some of these geological units have been dated at ca. 2.9 Ga (*Delhal and Ledent*, 1975; *Lasserre and Soba*, 1976; *Toteu et al.*, 1994). The Pan-African units rest directly on the Ntem complex basement and constitute the second cover of the Congo Craton. The first Craton cover (Proterozoic) is constituted by the Dja series and the tillitic complexes. It is discordant with the Mbalam belt and covered partially in the north by the Yaoundé nappe (*Mvondo et al.*, 2003; *Caron et al.*, 2010).

The major tectonic feature of the region is constituted by the extension of the Congo Craton under the Pan-African units. This event marks the subduction of the Congo Craton under the Pan-African belt. According to the hypothesis of subduction of the southern plate Craton, it must have provoked deep fractures in covers. However, the knowledge about the geodynamic and thermal structures in the area is limited and the geologic and tectonic data available are focused in the Mintom area, where a limestone deposit has been found by the mining inventory (*Vanhoutte and Salley*, 1986; *Vanhoutte*, 1989; *Caron et al.*, 2010). The present study deals with the application of

aeromagnetic data analysis to provide clues for productive zones of geothermal exploitation.

3 Previous geophysical studies

The most relevant geophysical studies were recently carried out in south-eastern Cameroon to delineate the major lineaments and the regional trends of structures affecting the area (Feumoe *et al.*, 2012), and to locate the buried faults in the basement and their depths (Ndougsa *et al.*, 2012). The depth of the faults range from 1 500 to 4 000 m and the shallower structures have a WSW-ENE trend. The main results improve our knowledge on the geological structures and geodynamic evolution of the South-East Cameroon. Spatial analysis of the lineaments map by Feumoe *et al.*, 2012, helped detecting morphological differences in the lineaments patterns. The southern sector of the map shows lineaments toward WNW-ESE trend. The northern and central sectors of the map show lineaments toward ENE-WSW (Fig. 2). According to Feumoe *et al.*, 2012, this configuration of aeromagnetic lineaments confirms the tectonic subdivision into the Congo Craton in the south and Pan-African or mobile belt in the north and helps identifying the deep tectonic boundary between them assigned to the major normal faults at the centre, indicating that it is a product of an active continental collision in the study area.

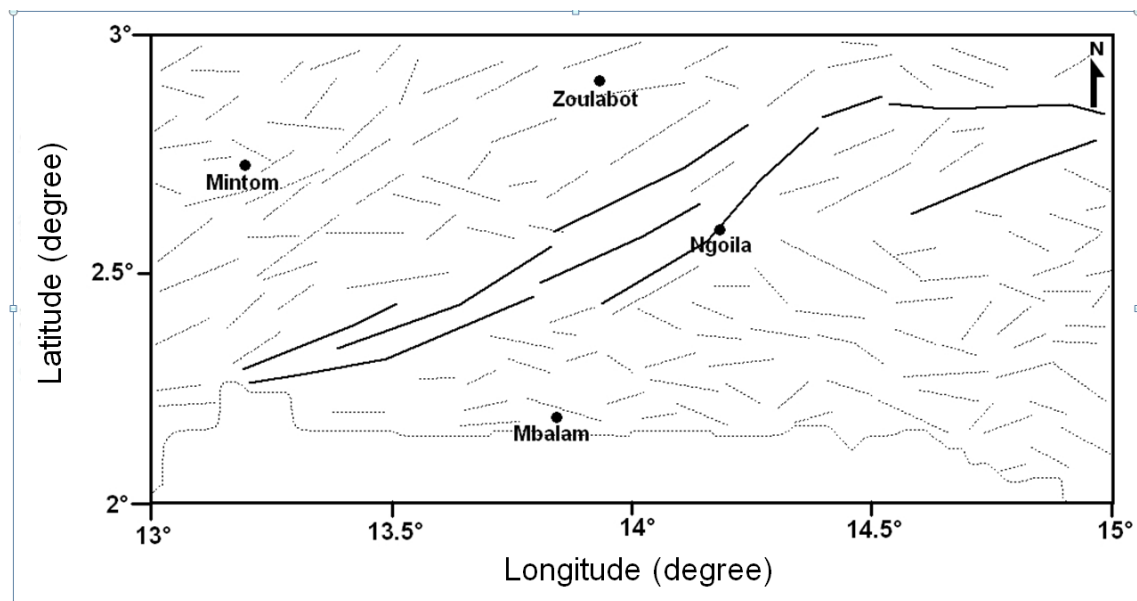


Fig. 2. Simplified tectonic map of the study area, showing regional features of the sub-surface (after Feumoe *et al.*, 2012).

According to Tokam *et al.* (2010), the joint inversion of Rayleigh wave group velocities and receiver functions suggest that: the Congo Craton is characterized by a crustal thickness of 43–48 km with an average crustal shear wave velocity of 3.9 kms^{-1} . The Congo Craton is underlain by the upper most mantle with an average shear wave velocity of 4.6 kms^{-1} . Beneath the CVL (Cameroon Volcanic Line) and the Neoproterozoic

mobile belt the results show similar crustal thickness of 35–39 km and velocity structure.

4 Data and processing methods

4.1 Aeromagnetic data

The aeromagnetic data were collected by the company SURVAIR (contractor) for the CIDA (client) in 1970. Aeromagnetic surveys were flown with a flight height of 235m and a nominal flight line spacing of 750 m in the direction N135°. After correcting the measurements for the temporal variations of the magnetic field, the total magnetic intensity (TMI) anomaly was obtained by subtracting the theoretical geomagnetic field or IGRF (International Geomagnetic Reference Field) at each station. The TMI anomaly data were then upward continued to a height of a mean altitude of 1 km before they were merged into a unified digital grid, which has a cell size of 0.01 degree (c. 1.1 km). This data grid was put at our disposal by the UK Geophysical Society GETECH Group Plc. The data are shown as a magnetic anomaly map for the South-East Cameroon in (Fig. 3). Subsequently, the total field aeromagnetic data were reduced to the east magnetic equator using FFTFIL (Fast Fourier Transform Filtering) program (Geosoft Oasis Montaj 6.4). The map of total magnetic field reduced to equator (Fig. 4) contains both long wavelength and small wavelength anomalies.

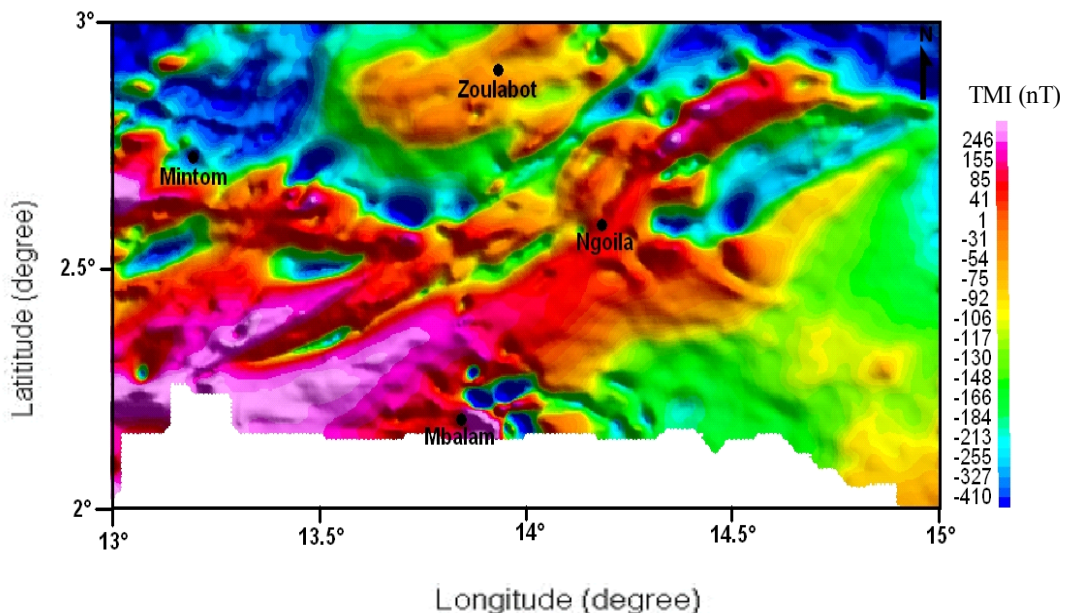


Fig. 3. Total magnetic intensity (TMI) anomaly map of the study area.

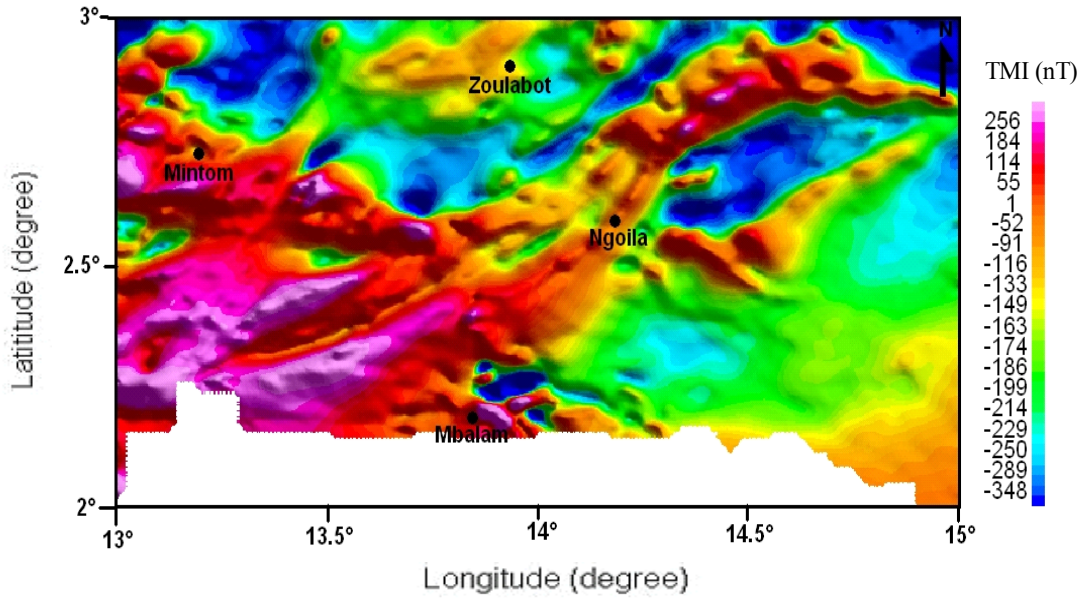


Fig. 4. Map of total magnetic intensity reduced to the equator (TMI-RTE).

4.2 Processing methods

The Fourier transform converts spatial data (magnetic grid) in to wave or frequency domain. The magnetic spectrum gives information on the depth of magnetic sources. Statistical estimation of depth to magnetic sources in the crust was described by *Spector and Grant* (1970). Their model assumed that magnetic sources are made up of independent ensembles of rectangular prisms which are characterized by frequency distribution of depth, width and length extent. Their assumption expects the value of the spectrum of the ensemble of sources to be the same as that of a single prism. The radial power spectrum is used to estimate the depth to the bottom (Z_b) of the magnetized bodies. This depth represents the CPD which is the transition depth of magnetic material to non-magnetic due to increased temperature.

$$\log(P(k)^{1/2}/|k|) = \log(A) - 2\pi \cdot Z_0 |k| \quad (1)$$

Where $P(k)$ is the radially averaged power spectrum of the anomaly, $|k|$ is the spatial wave number and A is a constant.

The second step is the estimation of the depth to the top boundary (Z_t) of the magnetic source from the slope of the line with the second longest wavelength (*Okubo et al.*, 1985),

$$\log(P(k)^{1/2}) = \log(B) - 2\pi \cdot Z_t |k| \quad (2)$$

Where B is a sum of constants independent of $|k|$. The basal depth (Z_b) of the magnetic source is then calculated from the equation:

$$Z_b = 2Z_0 - Z_t \quad (3)$$

Bottom depth (Z_b) can be estimated only if the centroid (Z_0) depth can be accurately determined. The obtained bottom depth of a magnetic source is assumed to be equal to the CPD.

Analysis of the CPD is one methods used to estimate the temperature gradients and the heat flow in the crust. Heat flow can be defined with the Fourier's law:

$$Q = K \frac{dT}{dz} \tag{4}$$

Where Q is the heat flow and K is the coefficient of thermal conductivity. In this equation, it is assumed that the direction of the temperature variation is vertical and the temperature gradient dT/dz is constant. According to *Tanaka et al. (1999)*, the Curie temperature (T_c) can be obtained from the Curie point depth (Z_b) and the thermal gradient dT/dz using the following equation:

$$T_c = Z_b \frac{dT}{dz} \tag{5}$$

Eqs. (4) and (5) give a relationship between the CPD (Z_b) and the heat flow (Q) as:

$$Q = K \frac{T_c}{Z_b} \tag{6}$$

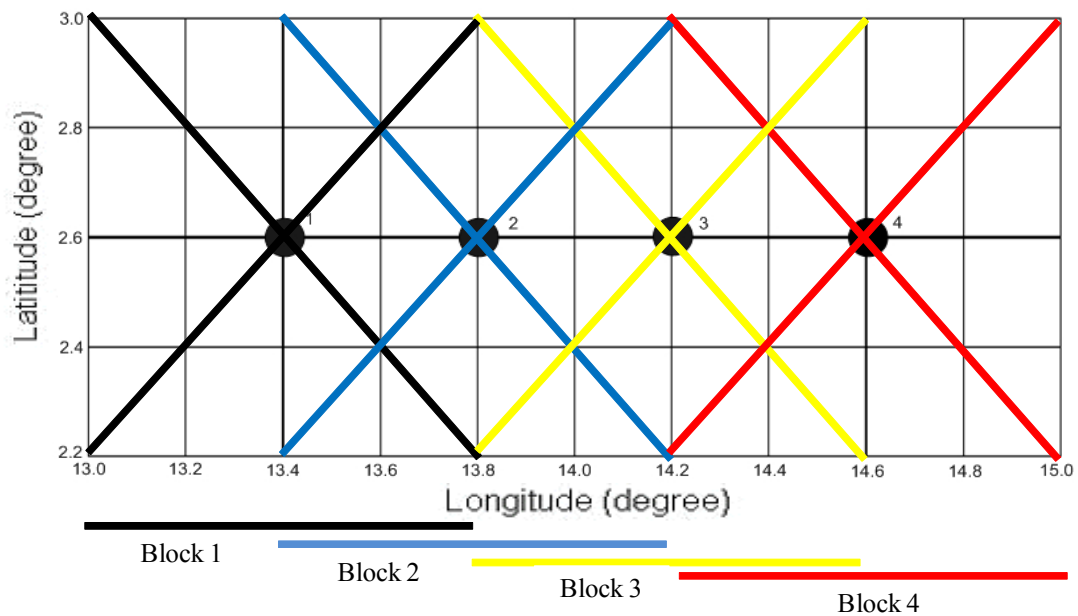


Fig. 5. Map showing the four overlapping blocks used for power spectral analysis. Each 89 km by 89 km block is denoted by a number at its centre.

5 Results

5.1 Estimation of the CPD

The methods for estimating the depth extent of magnetic sources are classified into two categories: those that examine the shape of isolated anomalies (*Bhattacharyya and Leu, 1975*) and those that examine the patterns of the anomalies (*Spector and Grant, 1970*). However, both methods provide the relationship between the spectrum of the magnetic anomalies and the depth to magnetic sources by transforming the spatial data into frequency domain. In this research, the later method was adopted. To obtain the CPD, spectral analysis of two-dimensional Fourier transform of the aeromagnetic data was made.

The spectral analysis was made using interactive FOURPOT program, (*Pirttijarvi, 2014*) which enables two-dimensional frequency domain processing of potential field data. The results of the analysis are plotted on a logarithmic scale against the radial wave number. On such a plot, if a group of sources has a same depth, they will fall onto a line of constant slope (tangent of the line fitted to the power spectra). Thus if there are sources at different depths, such as a shallow plutonic formation over a deep basement, the plot will be separated into two or more sections with different slope. The inverse of the angle of the slope is a measure of the depth of the source. This process was carried out to obtain the depth to the shallow (Z_t) and deep (Z_0) sources for the four sub-block (Fig. 6a-6d). The vertical dotted line represents the lower limit of the low-pass filter. This would hint that the spectrum values beyond the dotted line have been affected by the LP filter. The CPD for each block was then obtained using the Eq. (3). The results combined in Table 1 shows that the depth to the centroid (Z_0) ranges from 11.4 km to 13.8 km. The depth to the top boundary (Z_t) of magnetic sources ranges from 2.1 km to 3.0 km. The CPD varies between 20.0 and 25.0 km in the study area.

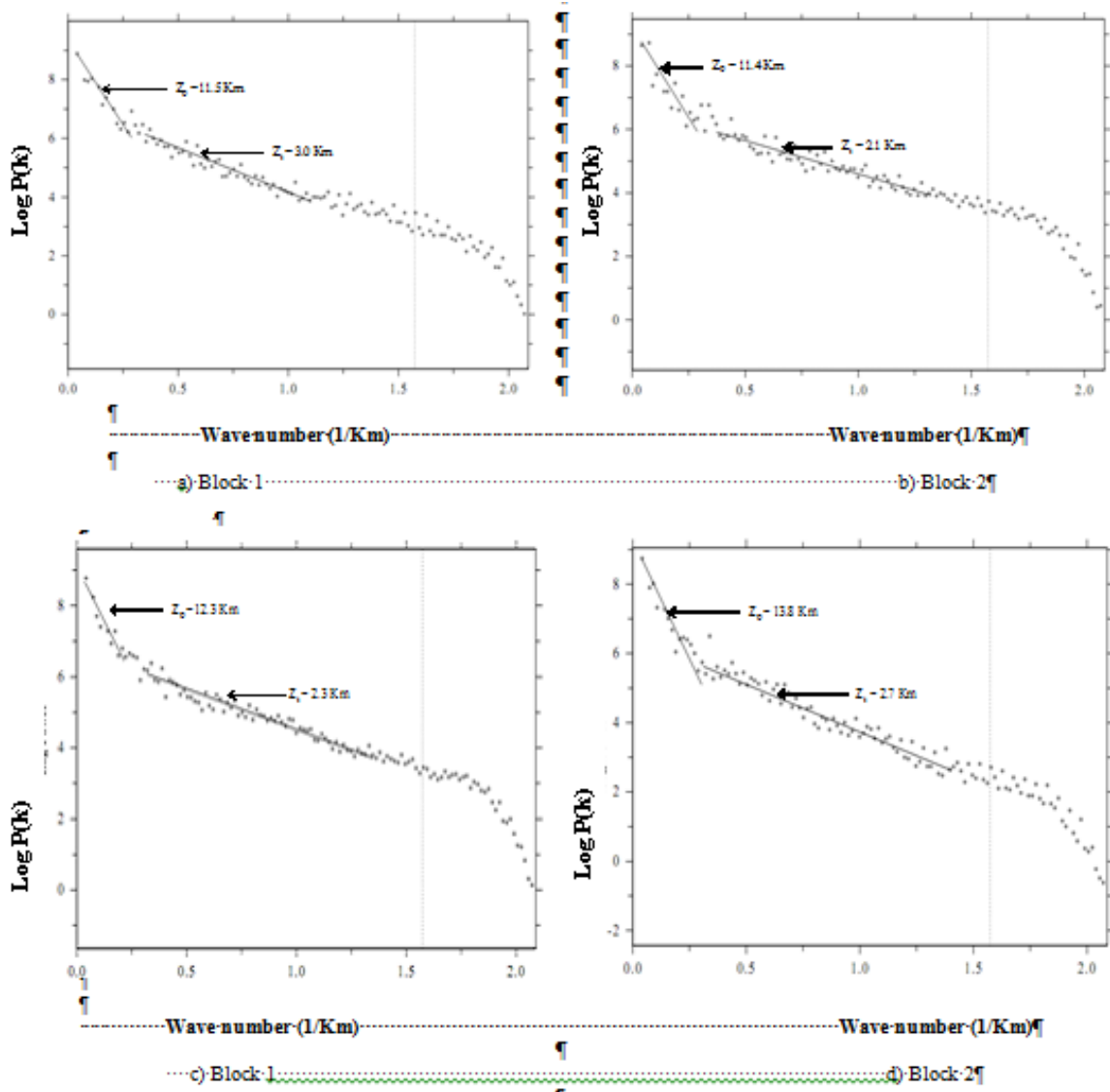


Fig. 6. Graphs of the logarithm of the radial power spectrum for the four blocks. *The tangents of the lines fitted to the power spectra using FOURPOT software are related to the depth to the sources Z_0 and Z_1 . The vertical dotted line shows the lower limit of low pass filter.*

5.2 Heat flow and thermal gradient estimates from CPD

CPD is inversely proportional to the heat flow as shown in Eq.(6) (Tanaka *et al.*, 1999; Stampolidis *et al.*, 2005). In this research, we used the Curie point temperature of 580 °C and the thermal conductivity of 2.5 Wm⁻¹°C⁻¹ as an average value for the igneous rocks over the basement. Derived heat flow and thermal gradient values are shown in Table 1. The heat flow varies from 57 and 72 mWm⁻² and the thermal gradient ranges between 23 and 29 °C/km. Considering an average value of 27°C/km for the study area, Eq. (4) suggests that the thermal conductivity values in the region vary between 2.1 and 2.7 W.m⁻¹.°C⁻¹. Table 1 shows that the heat flow decreases with increasing CPD. This almost linearly inverse relationship has been expressed in Fig. 7.

Table 1. Results of the spectral analysis, calculated average Curie point depth and estimates of the heat flow.

Blocks	Z ₀ (km)	Z _t (km)	CPD (km)	Geothermal gradient (°C/km)	Heat flow (mW/m ²)
1	11.5	3.0	20.0	29	72
2	11.4	2.1	20.7	28	70
3	12.3	2.3	22.3	26	65
4	13.8	2.7	25.0	23	57

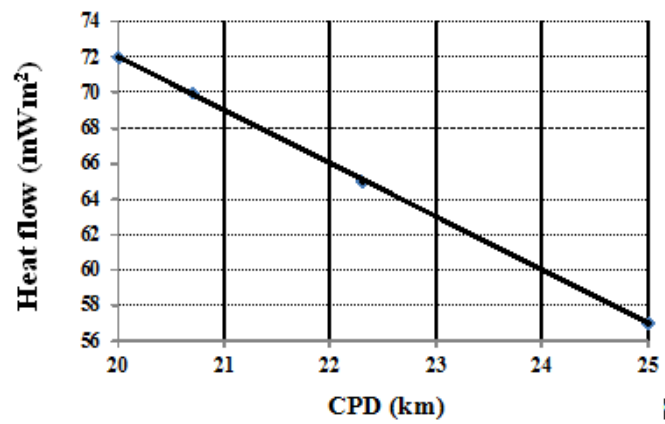


Fig. 7. Heat flow versus Curie point depth (CPD) in the study area.

6 Discussion of results

The magnetic anomalies reflect the episodic tectonics occurring in the study area and the changes in direction of anomalies are due to the variation in the direction and style of tectonics stress.

The CPD is greatly dependent upon geological conditions. CPDs are shallower than 10km for volcanic and geothermal fields, between 15-25 km for island arcs and ridges, deeper than 20 km in plateaus and trenches (*Tanaka et al.*, 1999). Generally, the units that comprise high heat flow values correspond to volcanic and metamorphic regions since these have high thermal conductivities. Additionally, tectonically active regions affect the Curie depth and the heat flow. In the study area, the obtained Curie depths and heat flows are consistent with the young metamorphic rocks.

6.1 CPD, heat flow and Moho

The investigation of the CPD isotherms and heat flow of the study area reveals that the CPD varies between 20.0 and 25.0 km and the heat flow is low being between 57 and 72 mWm⁻². The results are consistent with the active continental collision nature of the region marked by the subduction of the southern plate Craton and generally the

structural features that are considered to occur due to ENE-WSW extension in association with the Pan-African process.

The calculated CPD are further compared to the seismic Moho depth. The average Moho depth over the northern mobile belt (metamorphic formations in the study area) is 37 km whereas within the southern Craton (Precambrian formations in the study area) it is 46 km (*Tokam et al.*, 2010). Thus, this result shows that the CPDs are much lower than Moho depth values in the study area. The result obtained is similar to those derived from *Poudjom et al.*, (2013) study in the Adamawa area, using gravity investigation, where gravity model shows low thickness of the crust.

6.2 CPD and tectonic stability

Craton is a part of the lithosphere which has preserved the oldest formed crust. A thick magnetic crust is consistent with stable continental regions (e.g. craton and shield) while thin magnetic crust may conform to tectonically active region often associated with higher heat flow. From the estimated CPD we find that the magnetic crust is thickest in the East suggesting that this region is relatively more stable. Thus, it can be inferred that the south-eastern Cameroon is a region with low heat flow and forms stable continental shield region of the sub-continent.

7 Conclusion

The aeromagnetic anomaly of south-eastern Cameroon is mainly ENE-WSW and near E-W striking, with the dominant direction of ENE. The ENE-WSW trending anomaly represents the influence of the plate subduction which mainly reflects the collision between the southern plate Craton and the northern Pan-African mobile belt plate.

The CPDs are estimated by spectral analysis of magnetic anomaly data of south-eastern Cameroon. The results of the present investigation reveal that the Curie depth surface varies considerably beneath the area, reaching a value of 20.0 km in the west and a value of about 25.0 km in the east. The heat flow varies from 57 to 72 mWm⁻² and the thermal gradient ranges between 23 and 29 °C/km. The CPD is consistent with the prevailing geotectonic regime in the region, which is dominated by the subduction of the Congo Craton under the Pan-African plate in a roughly ENE-WSW direction. This study can be considered as a preliminary research aiming to improve our knowledge of the thermal regime of this complicated region as this area requires substantially more thermal data. On the other hand, despite its qualitative character, the positive correlation between CPDs, tectonic regime and surface heat flow supports the validity of analyzing regional aeromagnetic data to map CPDs on a regional scale.

Acknowledgments

We are grateful to GETECH Group plc (Leeds, UK) and its president and founder, Professor J.D. Fairhead for providing the aeromagnetic data used in this study.

References

- Abdelsalam, M.G., Liégeois, J.P. and Stern, R.J., 2002. The Saharan Metacraton, *J. Afr. Earth Sci.*, **34**, 119–136.
- Badalyan, M., 2000. Geothermal features of Armenia: a country update, Proceedings World Geothermal Congress, pp. 71–76, Kyushu-Tohoku, Japan.
- Bansal, A.R., G. Gabriel and V.P. Dimri., 2010. Depth to the bottom of magnetic sources in Germany analysis of anomalies of the Earth's magnetic total field, 8th Biennial International Conference and Exposition on Petroleum Geophysics.
- Banerjee, B., P.B.V. Subba Rao, Gautam Gupta, E.J. Joseph, and B.P. Singh., 1998. Results from a magnetic survey and geomagnetic depth sounding in the post-eruption phase of the Barren Island volcano, *Earth Planets Space*, **50**, 327–338.
- Basseka, C.A., 2002. Position tectonique, caractéristiques géophysiques et géochimiques des complexes précambriens au Sud-Cameroun, Thèse de Doctorat / PhD Thesis, *Univ. Russe de l'Amitié des Peuples*, 119 pp.
- Bhattacharyya, B.K. and L.K. Leu., 1975. Spectral analysis of gravity and magnetic anomalies due to two dimensional structures, *Geophysics*, **40**, 993–1013.
- Blakely, R.J., 1988. Curie temperature Isotherm Analysis and Tectonic Implications of Aeromagnetic Data from Nevada, *J. Geophys. Res.*, **93**, 11817–11832.
- Blakely, R. J. and S. Hassanzadeh., 1988. Estimation of depth to magnetic source using maximum entropy power spectra, with application to the Peru Chile Trench, in Nazca Plate: Crustal Formation and Andean Convergence, *Geolog. Soc. America Memoir*, **154**, 667–682.
- Byerly, P.E. and R.H. Stolt., 1977. An attempt to define the Curie point isotherm in northern and central Arizona, *Geophysics*, **42**, 1394–1400.
- Caron, V., Ekomane, E., Mahieux, G., Moussango, P. and Ndjeng, E., 2010. The Mintom formation (new): Sedimentology and geochemistry of neoproterozoic, paralic succession in south-east Cameroon. *J. Afr. Earth Sci.*, **57**, 367–385.
- Castaing, C., Feybesse, J.L., Thieblemont, D., Triboulet, C. and Chèvremont, P., 1994. Paleogeographical reconstructions of the Pan-African/Brasiliano orogen: closure of an oceanic domain or intracontinental convergence between major blocks. *Precambrian Res.*, **67**, 327–344, DOI:10.1016/0301-9268(94)90095-7.
- Connard, G., R. Couch and M. Gemperle, 1983. Analysis of aeromagnetic measurements from the Cascade Range in central Oregon, *Geophysics*, **48**, 376–390.
- Delhal, J. and L. Ledent, 1975. Données géochronologiques sur le complexe calcomagnésien du sud Cameroun. *Musée Royal d'Afrique Centrale*, Belgique. Rapp. Annuel, 71–75.
- Dolmaz, M.N., T. Ustaomer, Z.M. Hisarli and N. Orbay, 2005. Curie Point Depth variations to infer thermal structure of the crust at the African-Eurasian convergence zone, SW Turkey. *Earth Planets Space*. **57**, 373–383.
- Feumoe S.N.A., T. Ndougsa-Mbarga E. Manguelle-Dicoum and J.D. Fairhead, 2012. Delineation of tectonic lineaments using aeromagnetic data for the south-east Cameroon area. *Geofizika*, **29**, 175-192

- Feybesse, J.L., V. Johan, P. Maurizot and A. Abessolo, 1987. Evolution tectono-métamorphique libérienne et éburnéenne de la partie NW du craton zairois (SW Cameroun). In Matheis & Schandelmeier (eds), *Current Research in African earth sciences*, Balkema, Rotterdam, 9–13.
- Hisarli, Z.M., 1996. Determination of Curie Point Depths in Western Anatolia and Related with the Geothermal Areas, Ph.D. Thesis, Istanbul University, Turkey (Unpubl.), (in Turkish with English abstract).
- Lasserre, M. and D. Soba, 1976. Age Libérien des granodiorites et des gneiss à pyroxènes du Cameroun Meridional, *Bull. BRGM, Orleans*, **4**, 17–32.
- Manguelle-Dicoum, E.; Bokosah, A.S. and Kwende Mbanwi, T.E. 1992. Geophysical evidence for a major Precambrian schist–granite boundary in southern Cameroon. *Tectonophysics*, **205**, 437–446.
- Maurizot, P., A. Abessolo, J.L. Feybesse, V. Johan and P. Lecomte, 1985. Etude et prospection minière du sud-ouest Cameroun. Synthèse des travaux de 1978 à 1985, *Rapp. BRGM, Orleans*, 85 CMR 066, 274 pp.
- Mvondo, H., S.W.J. Den-Brok and J. Mvondo-Ondoa, 2003. Evidence for symmetric extension and exhumation of the Yaoundé nappe (Pan-African Fold Belt, Cameroon). *J. Afr. Earth Sci.*, **35**, 215–231.
- Nagata, T., 1961. *Rock Magnetism*, Maruzen, Tokyo, 350 pp.
- Ndougasa-Mbarga T., N.A.S. Feumoe, E. Manguelle-Dicoum and J.D. Fairhead, 2012. Aeromagnetic Data Interpretation to Locate Buried Faults in South-East Cameroon. *Geophysica*, **48**(1–2), 49–63.
- Nzenti, J.P., Barbey, P., Jegouzo, P. and Moreau, C., 1984. Un nouvel exemple de ceinture granulitique dans une chaîne protérozoïque de collision : Les migmatites de Yaoundé au Cameroun, *C. R. Acad. Sci. Paris*, **299**, 1197–1199.
- Okubo, Y., J.R. Graf, R.O. Hansen, K. Ogawa and H. Tsu, 1985. Curie point depths of the island of Kyushu and surrounding areas, Japan, *Geophysics*, **53**, 481–494.
- Okubo, Y., H. Tsu and K. Ogawa, 1989. Estimation of Curie point temperature and geothermal structure of island arc of Japan, *Tectonophysics*, **159**, 279–290.
- Okubo, Y. and T. Matsunaga, 1994. Curie point depth in northeast Japan and its correlation with regional thermal structure and seismicity, *J. Geophys. Res.*, **99**(B11), 22363–22371.
- Penaye, J., S.F. Toteu, W.R. Van Schmus and J.P. Nzenti, 1993. U-Pb and Sm-Nd preliminary geochronologic data on the Yaoundé series, Cameroon: Re-interpretation of the granulitic rocks as the suture of a collision in the “Centrafrican belt”, *C. R. Acad. Sci. Paris*, **317**, 789–794.
- Pirttijärvi, M., 2014. FOURPOT - Potential field data processing and analysis of using 2-D Fourier transform. User’s guide to version 1.3a. Department of Physics, University of Oulu, Finland
- Poidevin, J.L., 1983. La tectonique Pan-Africaine à la bordure nord du craton congolais : l’orogénèse des Oubanguides, in *Colloque on the African geology*, 12, Musée Royal de l’Afrique Centrale, Tervuren, Belgium. Abstract, 75.

- Shandini, N.Y., J.M. Tadjou, C.T. Tabod and J.D. Fairhead 2010. Gravity data interpretation in the northern edge of the Congo Craton, South-Cameroon. *Anuário do Instituto de Geociências* **33**(1), 73-82.
- Shuey, R.T., D.K. Schellinger, A.C. Tripp and L.B. Alley, 1977. Curie depth determination from aeromagnetic spectra, *Geophys. J. R. Astr. Soc.*, **50**, 75–101.
- Smith, R.B., R.T. Shuey, R.O. Freidline, R.M. Otis and L.B. Alley, 1974. Yellowstone Hot Spot: *New magnetic and seismic evidence*, *Geology*, **2**, 451–455.
- Smith, R.B., R.T. Shuey, J.R. Pelton and J.P. Bailey, 1977. Yellowstone hotspot: Contemporary tectonics and crustal properties from earthquake and aeromagnetic data, *J. Geophys. Res.*, **82**, 3665–3676.
- Spector, A. and F.S. Grant, 1970. Statistical models for interpreting aeromagnetic data, *Geophysics*, **35**, 293–302.
- Stampolidis, A. and G.N. Tsokas, 1981. Curie Point Depths of Macedonia and Thrace, N. Greece, *Pure and Appl. Geop.*, **159**, 2659–2671, 2002. S , eng or, A. M. C. and Y. Yılmaz, Tethyan evolution of Turkey: a plate tectonic approach, *Tectonophysics*, **75**, 181–241.
- Stampolidis, A., I. Kane, G.N. Tsokas and P. Tsourlo, 2005. Curie point depths of Albania inferred from ground total field magnetic data. *Surveys in Geophysics*. **26**, 461–480.
- Tadjou, J.M., R. Nouayou, J. Kamguia, H.L. Kande and E. Manguelle-Dicoum, 2009. Gravity analysis of the boundary between the Congo craton and the Pan-African belt of Cameroon. *Austrian Journal of Earth Sciences*, **102**(1), 71-79.
- Tanaka, A., Y. Okubo and O. Matsubayashi, 1999. Curie point depth based on spectrum analysis of the magnetic anomaly data in East and Southeast Asia, *Tectonophysics*, **306**, 461–470.
- Tchameni, R., K. Mezger, E.N. Nsifa and A. Pouclet, 2000. Neoproterozoic crustal evolution in the Congo Craton: Evidence from K-rich granitoids of the Ntem complex, southern Cameroon, *J. Afr. Earth Sci.*, **30**, 133–147, DOI: 10.1016/S0899-5362(00)00012-9.
- Tchameni, R., 2001. Crustal origin of Early Proterozoic syenites in the Congo Craton (Ntem Complex), South Cameroon, *Lithos*, **57**, 23-42.
- Trompette, R., 1994. Geology of Western Gondwana (2000–500 Ma): Pan-African–Braziliano aggregation of South America and Africa. *Balkema, Rotterdam*, 350 pp.
- Tsokas, G.N., R.O. Hansen and M. Fytikas, 1998. Curie point depth of Island of Crete (Greece), *Pure and Appl. Geop.*, **152**, 747–757.
- Telford, W.M., L.P. Geldart, R.E. Sherriff and D.A. Keys, 1990. Applied geophysics. Cambridge Univ. Press, Cambridge, 860 pp.
- Tokam A.P.K., C.T. Tabod, A.A. Nyblade, J. Julia, D.A. Wiens and M.E. Pasyanos, 2010. Structure of the crust beneath Cameroon, West Africa, from the joint inversion of Rayleigh wave group velocities and receiver functions, *Geophys. J. Int.*, **183**, 1061-1076.

- Toteu, S.F., W.R. Van Schmus, J. Penaye and J.B. Nyobé, 1994. U-Pb and Sm-Nd evidence for Eburnian and Pan-African high-grade metamorphism in cratonic rocks of southern Cameroon, *Precambrian Res.*, **67**, 321–347, DOI: 10.1016/0301-9268(94)90014-0.
- Vacquier, V. and J. Affleck, 1941. A Computation of average depth the bottom of the Earth's magnetic crust, based on a statistical study of local magnetic anomalies, *Trans. Amer. Geophys. Union*, **22**, 446–450.
- Vanhoutte, M., 1989. Bilans de l'étude géologique et l'évaluation des calcaires de Mintom. Projet de mise en valeur d'indices miniers sélectionnés. United Nations Development Program, (*Unpublished report, 92*), 64 pp.
- Vanhoutte, M. and P. Salley, 1986. Reconnaissance des calcaires de Mintom. Projet de recherches 1045 minières, sud-est Cameroun. United Nations Development Program, (*Unpublished report, 91*), 59 pp.